Reeves, et al., in AGU Monograph on Resolution of Processes in Space and Time,
J. L. Burch and J. H. Waite, Jr., eds, 149, 1993.

The Structure and Dynamics of the Plasma Sheet During the Galileo Earth-1 Flyby

G. D. Reeves, T. A. Fritz, and R. D. Belian

Los Alamos National Laboratory, Los Alamos, NM 87545

R. W. McEntire, D. J. Williams, and E. C. Roelof

The John's Hopkins University Applied Physics Laboratory, Laurel, MD

M. G. Kivelson

University of California, Los Angeles, CA

B. Wilken

Max Planck Institut für Aeronomie, Katlenburg-Lindau, Germany

The flyby of the Earth by the Galileo spacecraft on December 8, 1990 provided an excellent opportunity to study the spatial structure and temporal dynamics of the near-Earth plasma sheet. From 1700 to 2000 UT, when Galileo was within R < 20 R_E, the magnetotail was in a stretched configuration. Galileo's trajectory was ideal for investigating spatial structure in the tail. We identified periods in which Galileo was in the plasma sheet, in the trapping boundary for keV particles, and in the stable radiation belts. Geosynchronous spacecraft 1984-129 monitored the temporal dynamics at fixed radius. We compared temporal dynamics at Galileo and at geosynchronous orbit. Both spacecraft saw a long-term decline in energetic particle fluxes which appears to have been a purely temporal change. Only 1984-129 observed two more traditional, and dramatic, growth phase dropouts illustrating temporal changes confined to one spatial region. In the plasma sheet Galileo did not observe flux variations due to radial gradients but did observe temporal variations caused primarily by flapping of the tail or magnetic reconfiguration. One sequence of such variations caused the spacecraft to enter and exit the trapping boundary region quite close to the earth. When Galileo was near spacecraft 1984-129 the two spacecraft observed very different fluxes which implies the presence of very strong spatial gradients in that region of space.

INTRODUCTION

It is a well-known quandary in space plasma physics that it is generally impossible to distinguish between spatial structures and temporal processes using single-point measurements. Indeed, even with measurements from multiple spacecraft one is rarely fortunate enough to have the spacecraft in the right places at the right time. The Galileo Earth-1 flyby on December 8, 1990 was one of those serendipitous occasions. Galileo's trajectory was designed to use the Earth's gravity to propel it on its way to Jupiter. Fortunately for our purposes this trajectory also allowed Galileo to rapidly sample spatial structures in the magnetotail. At the same time spacecraft 1984-129 monitored the midnight local time sector at geosynchronous altitudes. It's orbit, at a fixed radius, is well suited to observe temporal variations. Galileo's passage through the magnetotail required several hours and thus was too slow to provide a "snapshot" of the magnetosphere. This is particularly true since the flyby occurred during an active period. However the combined data from Galileo and from 1984-129 allowed us to separate spatial and temporal effects and to study the structure and dynamics of the plasma sheet when it was in a stretched, growth phase configuration. (See *Kivelson et al.* [1993] for an overview of the Earth-1 flyby.)

Instruments

The Galileo spacecraft carries a complement of field and particle instruments. In this study we have used data from the fluxgate magnetometer (described in detail by *Kivelson et al.* [1992]) and the energetic particle detector (EPD) [*Williams et al.*, 1992]. The low-energy magnetospheric measurement system (LEMMS) of the Galileo energetic particle detector measures electrons and protons with energies of tens of keV. The channels used for this study are the A0–A5 channels that measure protons in differential energy bins with energies of 22–42, 42–65, 65–120, 120–280, 280–515, and 515–825 keV; and the E0–E3 and F0 channels that measure electrons in differential energy bins with energies of 15–29, 29–42, 42–55, 55–93, and 93–188 keV. In this study we use spin-averaged LEMMS data. The spin period of Galileo is approximately 20 s. In order to obtain full unit sphere coverage the EPD is also articulated with respect to the spin plane. A stepper motor moves the sensors in the plane containing the spin axis after each spin. When the particle distribution is not isotropic this adds a modulation to the EPD data that has not been removed. Although the number of steps is controllable, during the Earth-1 flyby the modulation period is approximately 200 s.

Spacecraft 1984-129 was one of a continuously operating constellation of three geosynchronous spacecraft that carried Los Alamos charged particle analyzer (CPA) instruments from 1976 to the present. The CPA includes two instrument sub-systems. The LoE sub-system measures electrons in six nested energy channels with low-energy thresholds of 30, 45, 65, 95, 140, and 200 keV. All share a common high energy limit of 300 keV. The LoP subsystem has ten channels with thresholds of 72, 91, 104, 125, 153, 190, 235, 292, 365, and 475 keV. The common upper energy limit is 573 keV. Although both instruments have 256 ms resolution, throughout this paper we use data that were averaged over all telescopes, 6 spins (approximately 1 minute), and therefore over the unit sphere. Differential energy measurements are obtained from the nested energy measurements by subtracting adjacent channels. More information on the CPA detectors can be found in the paper by *Higbie et al.* [1978].

OBSERVATIONS

Figure 1 shows the trajectories of Galileo and spacecraft 1984-129. The top plot shows the trajectories projected into the equatorial plane for times between 1700 and 2000 UT. Both spacecraft were in the midnight sector. Galileo's trajectory was nearly radial and 1984-129's was azimuthal. Galileo crossed the geosynchronous drift shell at 1917:30 UT, at which time the spacecraft were separated by approximately 2.5° in azimuth. The bottom plot shows the trajectories as a function of Z_{GSM} and radius. In this coordinate system spacecraft 1984-129 is nearly motionless over this 3-hour period. Also shown are field line traces according to the *Tsyganenko* [1989] field model for its most stretched configuration (Kp > 4+). The field lines are traced starting at the position of the Galileo spacecraft at 15-minute intervals. The shading of the Galileo trajectory shows the magnetotail regions measured at different locations along the trajectory and is discussed in the following section.

We show the fluxes of energetic particles measured by Galileo and 1984-129 between 1700 and 2000 UT in Figure 2. The top panel shows electrons and the bottom panel shows protons. We have only plotted one energy range for each species and chose similar energy ranges for both spacecraft. The fluxes in other energy ranges show similar features and are plotted in *Reeves et al.* [1993]. The universal time and the position of the two spacecraft are indicated along the bottom of the plot and the fluxes measured at the two spacecraft are plotted on the same scale.

Between 1700 and 2000 UT the fluxes of both protons and electrons at geosynchronous orbit declined by almost two orders of magnitude. Superimposed upon that long-term decline were two dropouts of approximately 30 min duration. The first dropout began at approximately 1730 UT. The proton and electron fluxes both returned at 1811 UT but did not attain their previous levels. The second dropout was observed primarily in the electron fluxes. This is because the proton fluxes measured by 1984-129 were already near the 1-count level and lower fluxes could not be recorded. The second dropout began at approximately 1912 UT. It intensified at 1927 UT and recovery was at 1941 UT. The final recovery (and injection) of energetic particles at geosynchronous orbit was not recorded until 2053 UT, after the period of interest for this study.

The Galileo energetic particle fluxes were quite different. The only feature that was similar to the geosynchronous energetic particle fluxes was a gradual decline in flux levels observed between 1700 and 1841 UT. The similarity is particularly apparent in the proton fluxes in the lower panel of Figure 2. The Galileo and geosynchronous fluxes track each other quite closely in that interval except during the first geosynchronous dropout when the Galileo electron fluxes increased. The Galileo proton fluxes were unaffected. At 1811 UT when the geosynchronous particle fluxes recovered there was little change at Galileo except a small injection of electrons. Between 1825 and 1841 UT three narrow spikes were observed in the Galileo electron fluxes. They are the result of modulation caused by the LEMMS stepper motor combined with a very anisotropic pitch angle distribution. A more dramatic change in flux levels was recorded by Galileo at 1841 UT when the flux levels increased by approximately an order of magnitude and remained high. Between 1841 and 1917 UT the Galileo fluxes were highly variable. Peak Galileo electron and proton fluxes were comparable to the fluxes measured by 1984-129 at geosynchronous orbit. After 1917:30 UT the Galileo fluxes were higher than those measured by 1984-129 and the fluxes were not highly variable.

Figure 3 shows the Galileo magnetometer measurements [*Kivelson et al.,* 1992, 1993] along with the Galileo electron fluxes. From 1700 to about 1747 UT B_x was quite small and varied in sign indicating that Galileo was very close to the neutral sheet, as expected from its orbit (Figure 1). After about 1747 UT when B_x was uniformly positive, the inclination of the field (□) was close to 90°, indicating that the field was in a highly stressed, tail-like configuration. The increasing field magnitude was a result of Galileo's motion toward the Earth. Two intervals have been shaded. During those times both the field components and the particle fluxes were variable. The first of these intervals occurred during the first geosynchronous dropout and the second spans the interval between 1841 and 1917 UT discussed above. Close examination shows that the peak particle fluxes are correlated with minimums in the field intensity suggesting that the flux variations may be due to apparent motion of the spacecraft across magnetic flux surfaces. (The three energetic electron peaks between 1825 and 1841 UT were not included in the shaded portion of Figure 3 because they are caused by instrumental effects, not temporal variability.) Interestingly the recovery of fluxes at geosynchronous orbit and the small injection of electrons at Galileo at 1811 UT were not accompanied by any variation in the magnetic field magnitude or direction. In particular, no "dipolarization" of the field was observed.

ANALYSIS

The Galileo energetic particle signatures during the three hours analyzed in this study can be used to identify three spatial regions: the plasma sheet, the trapping boundary, and the radiation belts. At the beginning of the interval Galileo was clearly in the plasma sheet. (In this study we do not distinguish between the plasma sheet and the plasma sheet boundary layer.) At the end of the interval it is equally clear that Galileo was in the radiation belts. Below we identify the interval between 1841 and 1917 UT as the period of interaction with the trapping boundary. In Figure 1b we use shading of the Galileo trajectory to indicate where Galileo was when it measured each of these regions. A vertical-striped line indicates the plasma sheet (before 1841 UT), the black line indicates the trapping boundary (1841-1917:30 UT), and the horizontal-striped line indicates the stable radiation belts (after 1917:30).

1700–1841 UT

Between 1700 and 1841 UT, while Galileo was in the plasma sheet, 1984-129 recorded a growth phase energetic particle dropout. This dropout of energetic particles was examined in detail by *Reeves et al.* [1993] who concluded that it was consistent with the traditional interpretation of growth phase signatures of magnetotail thinning [e.g., *Hones et al.,* 1967, 1973; *Baker et al.,* 1981; *Baker and McPherron,* 1990; *Lui,* 1991]. Magnetotail thinning causes magnetic flux tubes to move across the spacecraft. Hence the spacecraft becomes connected to field lines that map further down the tail and therefore to a region of lower fluxes. If the thinning is extreme the trapping boundary can move across the spacecraft as appears to be the case here.

Magnetotail thinning is caused by an intensification of the cross-tail current and is therefore primarily a temporal phenomenon. It is also expected to affect a large portion of the magnetotail. However, neither dropout was observed by Galileo. For the second dropout Galileo was inside geosynchronous orbit in the radiation belts, but the first dropout occurred when Galileo was at 13–15 R_E. The fact that Galileo did not observe this dropout suggests that its effects were probably confined to the trapping region. In other words, while the tail may have thinned both at geosynchronous orbit and at Galileo's position, the necessary radial gradient of energetic particle fluxes did not exist in the plasma sheet though it did exist between the trapping region and the plasma sheet.

Comparison of the fluxes measured by Galileo and 1984-129 provide direct evidence of the gradient between geosynchronous orbit and the plasma sheet (Figure 2) but, we can only infer the lack of such a gradient in the plasma sheet proper. Supporting evidence is seen during the deepest part of the dropout. From approximately 1745 to 1811 UT the fluxes measured by Galileo and 1984-129 were nearly equal (Figure 2). This was true for both protons and electrons at all measured energies (data not shown). Even some of the temporal variations in the electron fluxes during the dropout were seen by both spacecraft. While it is likely that the field line connected to 1984-129 mapped to the plasma sheet it is highly unlikely that it mapped to the same radius or the same local time as Galileo (Figure 1a). Therefore the equality of the fluxes during the dropout suggests some uniformity in the level of energetic particle fluxes in the plasma sheet during this time. The temporal variations seen by both spacecraft during the deepest part of the dropout were correlated with magnetic field variations (Figure 3) and hence may be the result of flapping of the magnetotail.

1841–1917:30 UT

At 1841 UT an abrupt change in the Galileo energetic particle fluxes was observed. The 1841 UT transition clearly had a temporal as well as a spatial character. At that time there was a marked decrease in B_x and $|B|$ and an increase in B_y indicating both a rotation and a relaxation of the field. From 1841 to 1917 UT both the particle fluxes and magnetic field measured by Galileo were highly variable (Figure 3). The highest fluxes were measured when B_x (and therefore $|B|$) was lowest. At those times the field was slightly less tail-like. Also at those times the Galileo energetic particle fluxes were comparable in magnitude to the fluxes measured by 1984-129. Therefore, during times of peak fluxes, Galileo was probably in the same flux region as 1984-129, namely the trapping region for keV particles. At other times the Galileo fluxes were significantly lower than those measured by 1984-129. Therefore we suggest that between 1841 and 1917 UT Galileo skimmed along the trapping boundary and that "flapping" of the magnetotail moved that boundary moved across the spacecraft causing the variations in the measured magnetic field and particle fluxes.

The interval during which Galileo was in the trapping boundary is particularly interesting because of its implications for the structure of the magnetotail. We have seen that Galileo moved in and out of the trapping boundary and therefore conclude that the trapping boundary was nearly parallel to the Galileo trajectory. This, in turn, implies that the magnetic flux surfaces were nearly parallel to the Galileo trajectory. While the Tsyganenko model predicts that Galileo flew nearly along the magnetic field from 1800 to about 1830 UT, by 1900 UT the Tsyganenko model predicts that Galileo should have been rapidly crossing flux surfaces. One can see from Figure 1, though, that if the magnetotail were "squeezed" in the vicinity of 6–10 R_E that Galileo's trajectory could have been more parallel to the flux surfaces. The conclusion that the Tsyganenko model is not sufficiently stretched at distances of 6–10 R_E has been reached before based on magnetic field measurements alone [*Kaufmann,* 1988], but here we see direct evidence of the effect of magnetotail thinning on the structure of energetic particle drift shells.

1917:30–2000 UT

Reeves et al. [1993] determined that Galileo crossed the geosynchronous drift shell at 1917:30 UT. At that time the fluxes of electrons were equal at the two spacecraft for all measured energies. After that time Galileo measured fluxes which were higher than those measured by 1984-129. The fluxes measured after 1917:30 showed little variability other than that expected as Galileo moved from high to low altitudes. Therefore we identify the region sampled between 1917:30 and 2000 UT as the stable radiation belts.

It is interesting to contrast the two transitions at 1841 UT and at 1917:30 UT. At 1917:30, as Galileo crossed the geosynchronous drift shell, the electron fluxes increased abruptly. Unlike the 1841 UT transition, the abruptness does not appear to have been due to a temporal change. Spacecraft 1984-129 remained at fixed radius and observed a continuing growth phase dropout as the Galileo fluxes increased. Since the two spacecraft were in such close proximity one would expect a temporal change to be apparent in both data sets. Furthermore, the Galileo protons did not experience a similar abrupt increase and there was no signature in the Galileo magnetometer data. Therefore we attribute this transition to the presence of a strong gradient in the energetic electron fluxes in the vicinity of geosynchronous orbit. (*Reeves et al.* [1993] have examined this gradient in more detail.) Hence the Galileo data show that the region in which growth phase dropouts are observed is limited to a region with both an inner boundary and an outer boundary. The outer boundary is the trapping boundary. The inner boundary must be defined by where magnetotail thinning does or does not cause particle gradients to move across the spacecraft. These results suggest that boundary may have been very near geosynchronous orbit and was highly localized in azimuth, radius, or latitude.

CONCLUSIONS

We have examined the structure and dynamics of the magnetotail during the Galileo Earth-1 flyby. We determined the times in which Galileo was in the plasma sheet, the trapping boundary, and the radiation belts. The measurements suggest that Galileo's trajectory skimmed the trapping boundary and that variations in the magnetic field caused that boundary to pass back and forth across the spacecraft. A comparison of the shape of the magnetic field predicted by the Tsyganenko model with the measurements of the trapping boundary show that the actual magnetic field was much more tail-like than the model field, especially at distances of 6–10 R_E.

A long-duration decline of energetic particle fluxes was observed both by 1984-129 at geosynchronous orbit and by Galileo in the plasma sheet. Superimposed on that feature were two growth phase dropouts of energetic particle fluxes at geosynchronous orbit. The first occurred when Galileo was in the plasma sheet and the second occurred when Galileo was entering or within the radiation belts. Since neither dropout was observed by Galileo we concluded that the effects magnetotail thinning that produced the dropouts at geosynchronous orbit were limited to the trapping region. We also found that during the first dropout the fluxes measured by 1984-129 became nearly equal to those measured by Galileo even though it is highly unlikely that the field connected to 1984-129 mapped to the vicinity of Galileo. Therefore we concluded that the energetic particle gradients in the plasma sheet during this time were relatively small and that the variations in energetic electron fluxes which were observed at that time were probably related to a flapping motion of the magnetotail. We compared the two boundary crossings identified in the Galileo data and concluded that the transition from the plasma sheet to the trapping boundary was caused by a reconfiguration of the magnetic field while the transition from the trapping boundary to the radiation belts occurred due to Galileo's motion alone, without temporal variation.

The combination of data from a fast-moving spacecraft in the plasma sheet and a slow-moving geosynchronous spacecraft near local midnight was a vital asset for this study. We look forward with anticipation to similar studies which should be possible utilizing Los Alamos geosynchronous and Geotail data.

Acknowledgments: This work was supported by the U.S. Department of Energy Office of Basic Energy Sciences. Work at UCLA was partially supported by the Jet Propulsion Laboratory under contract JPL-958694. The authors would like to thank Tom Armstrong, Vassilis Angelopoulos, Alan Roux, Lou Frank, Tom Cayton, and Bob McPherron for their insights and enthusiasm.

REFERENCES

Baker, D. N. and R. L. McPherron, Extreme energetic particle decreases near geostationary orbit: A manifestation of current diversion within the inner plasma sheet, *Adv. Space Res., 10,* 131, 1990.

Baker, D. N., E. W. Hones, P. R. Higbie, R. D. Belian, and P. Stauning, Global properties of the magnetosphere during a substorm growth phase: A case study, *J. Geophys. Res., 86,* 8941, 1981.

Higbie, P. R., R. D. Belian, and D. N. Baker, High-resolution energetic particle measurements at 6.6 R_E 1, Electron micropulsations, *J. Geophys. Res., 83,* 4851, 1978.

Hones, E. W., J. R. Asbridge, S. J. Bame, and I. B. Strong, Outward flow of plasma in the magnetotail following geomagnetic bays, *J. Geophys. Res., 72*, 5879, 1967.

Hones, E. W., J. R. Asbridge, S. J. Bame, and S. Singer, Substorm variations of the magnetotail plasma sheet from X-sm≈-6 R_E to X-sm≈60 R_E, *J. Geophys. Res., 78*, 109, 1973.

Kaufmann, R. L., Substorm currents: growth phase and onset, *J. Geophys. Res., 92*, 7471-7486, 1987.

Kivelson, M. G., K. K. Khurana, J. D. Means, C. T. Russell, and R. C. Snare, The Galileo magnetic field investigation, *Space Sci. Rev., 60,* 357, 1992.

Kivelson, M. G., C. F. Kennel, R. L. McPherron, C. T. Russell, D. J. Southwood, R. J. Walker, K. K. Khurana, P. J. Coleman, C. M. Hammond, V. Angelopoulos, A. J. Lazarus, R. P. Lepping, and T. J. Hughes, The Galileo Earth encounter: Magnetometer and allied measurements, *J. Geophys. Res., 98,* 11,299, 1993.

Lui, A. T. Y., A synthesis of magnetospheric substorm models, *J. Geophys. Res., 96*, 1849, 1991.

Reeves, G. D., T. A. Fritz, R. D. Belian, R. W. McEntire, D. J. Williams, E. C. Roelof, M. G. Kivelson, and B. Wilken, Structured plasma sheet thinning observed by Galileo and 1984-129, *J. Geophys. Res., 98*, 21,323, 1993.

Tsyganenko, N. A., A Magnetospheric magnetic field model with a warped tail current sheet, *Planet. Space Sci, 37,* 5, 1989.

Williams, D. J., R. W. McEntire, S. Jaskuler, and B. Wilken, The Galileo energetic particle detector, *Space Sci. Rev., 60,* 385, 1992.

Reeves, et al., in AGU Monograph on Resolution of Processes in Space and Time,
J. L. Burch and J. H. Waite, Jr., eds, 149, 1993.

R. D. Belian, T. A. Fritz, and G. D. Reeves, Los Alamos National Laboratory, NIS-2, Mail Stop D-436, Los Alamos, NM 87545.

M. G. Kivelson, University of California, Los Angeles, CA 90024.

R. W. McEntire, E. C. Roelof, and D. J. Williams, The Johns Hopkins University Applied Physics Laboratory, Laurel, MD 20723.

B. Wilken, Max-Planck-Institut für Aeronomie, Postfach 20, D-3411 Katlenburg-Lindau, Germany

FIGURE CAPTIONS

Fig. 1. The trajectories of Galileo and geosynchronous spacecraft 1984-129. Positions are marked for each hour from 1700 to 2000 UT. (A) The trajectories in the X-Y plane. Galileo made a nearly radial pass through the midnight sector while 1984-129 made an azimuthal pass. At 1917:30 UT Galileo crossed the geosynchronous orbit within 2.5° longitude of the position of 1984-129. (B) The Galileo trajectory plotted as a function of Z-GSM and Radius, $(X^2+Y^2+Z^2)^{1/2}$. In this coordinate system 1984-129 is nearly motionless over this 3-hour period. Also shown are the magnetic field lines connected to Galileo at each 15 minute interval as predicted by the *Tsyganenko* [1989] model for Kp>4+. The trajectory of Galileo is plotted with shaded lines representing the magnetotail regions measured by Galileo (see text).

Fig. 2. A comparison of geosynchronous (shaded line) and Galileo (solid line) fluxes. Electrons are shown in the top panel and protons are shown in the bottom panel. For electrons, the Galileo LEMMS and 1984-129 CPA instruments had very similar energy bands so a direct flux comparison can be made. For protons, three energy bands from the 1984-129 CPA instrument have been added together to show the flux from 72 to 125 keV which can be compared with the Galileo LEMMS fluxes from 65 to 120 keV.

Fig. 3. A comparison of energetic electron fluxes with data from the UCLA magnetometer on Galileo. The top panel shows 29–42 keV electron fluxes (in counts/cm^2/s/sr/keV) and the lower panel shows all three components of the magnetic field (in nT), its magnitude (in nT), and the inclination angle of the field (□=tan^{-1}(B_x/B_z)). The shaded areas show periods of particle and magnetic field variability.

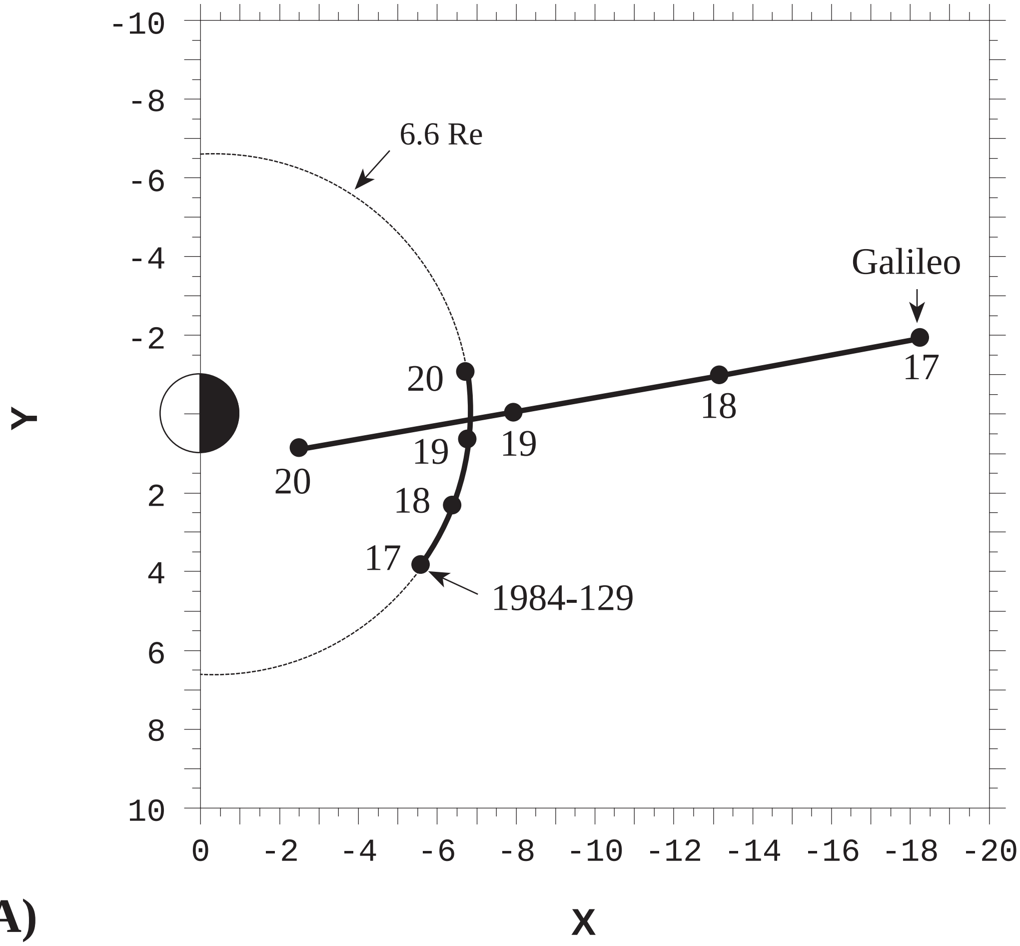
6.6 Re
Galileo
20
17
18
19
19
20
18
17
1984-129
Y
X
-10
-8
-6
-4
-2
2
4
6
8
10
0
-2
-4
-6
-8
-10
-12
-14
-16
-18
-20

(A)

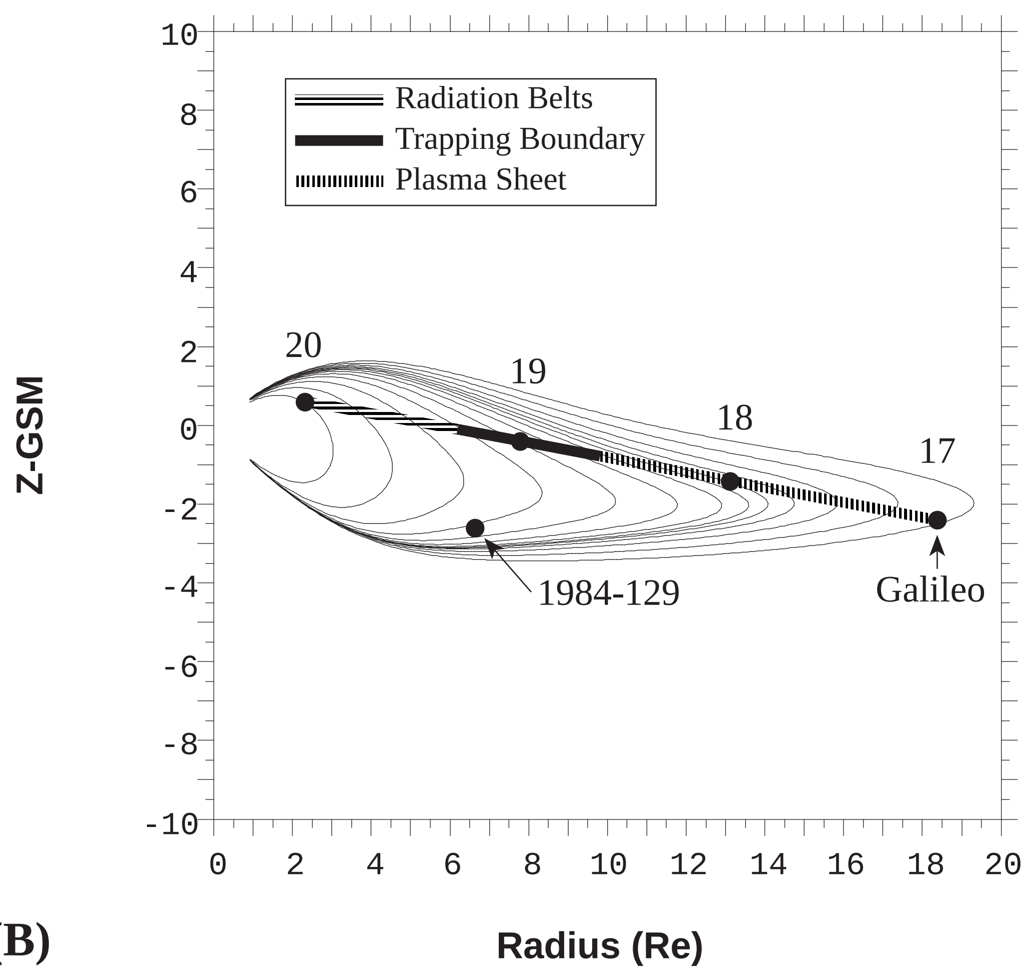
Radiation Belts
Trapping Boundary
Plasma Sheet
20
19
18
17
1984-129
Galileo
Z-GSM
Radius (Re)
10
8
6
4
2
0
-2
-4
-6
-8
-10
0
2
4
6
8
10
12
14
16
18
20

(B)

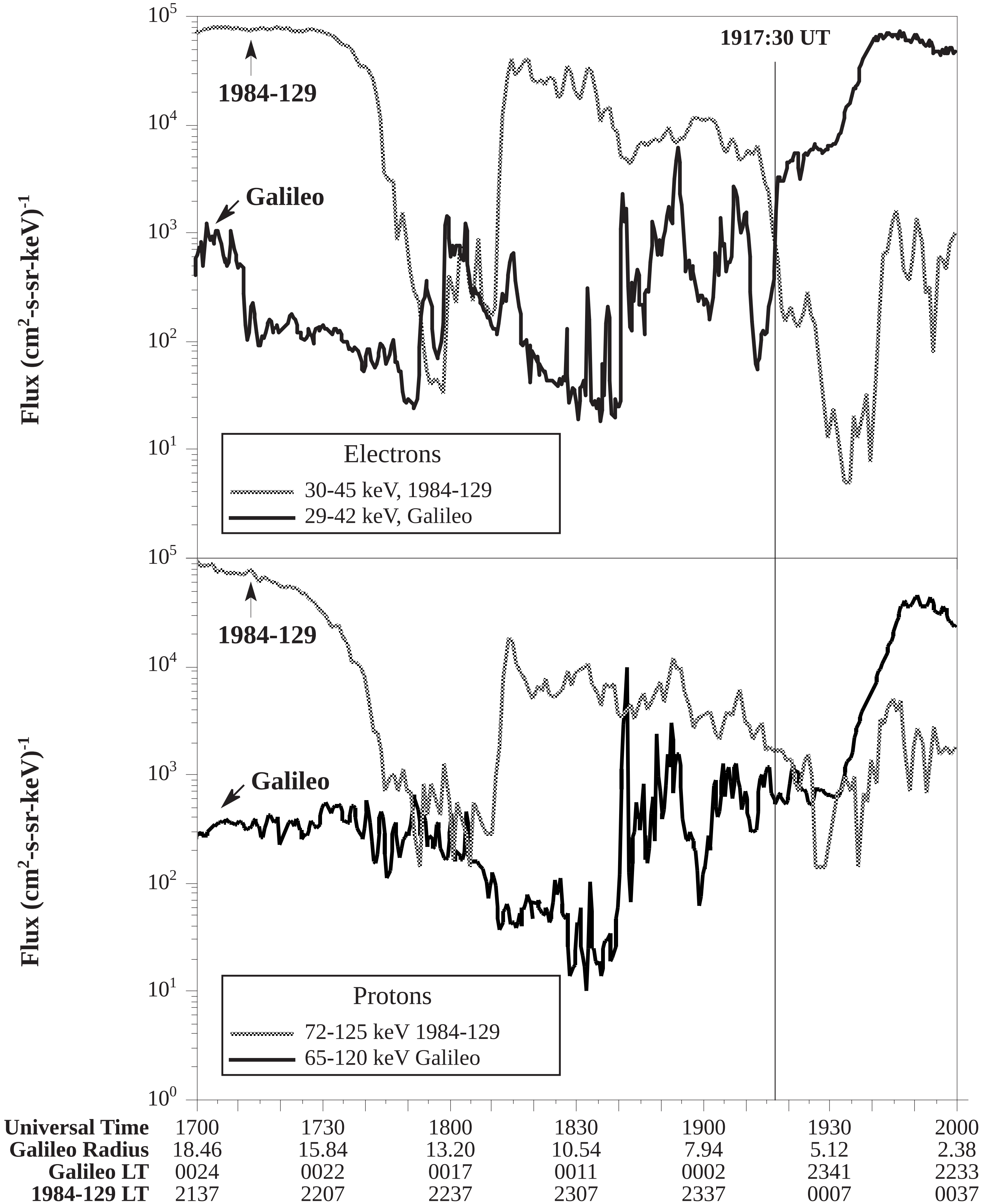

Flux (cm2-s-sr-keV)-1
10^5
10^4
10^3
10^2
10^1
1984-129
Galileo
1917:30 UT
Electrons
30-45 keV, 1984-129
29-42 keV, Galileo
Flux (cm2-s-sr-keV)-1
10^5
10^4
10^3
10^2
10^1
10^0
1984-129
Galileo
Protons
72-125 keV 1984-129
65-120 keV Galileo
Universal Time 1700 1730 1800 1830 1900 1930 2000
Galileo Radius 18.46 15.84 13.20 10.54 7.94 5.12 2.38
Galileo LT 0024 0022 0017 0011 0002 2341 2233
1984-129 LT 2137 2207 2237 2307 2337 0007 0037

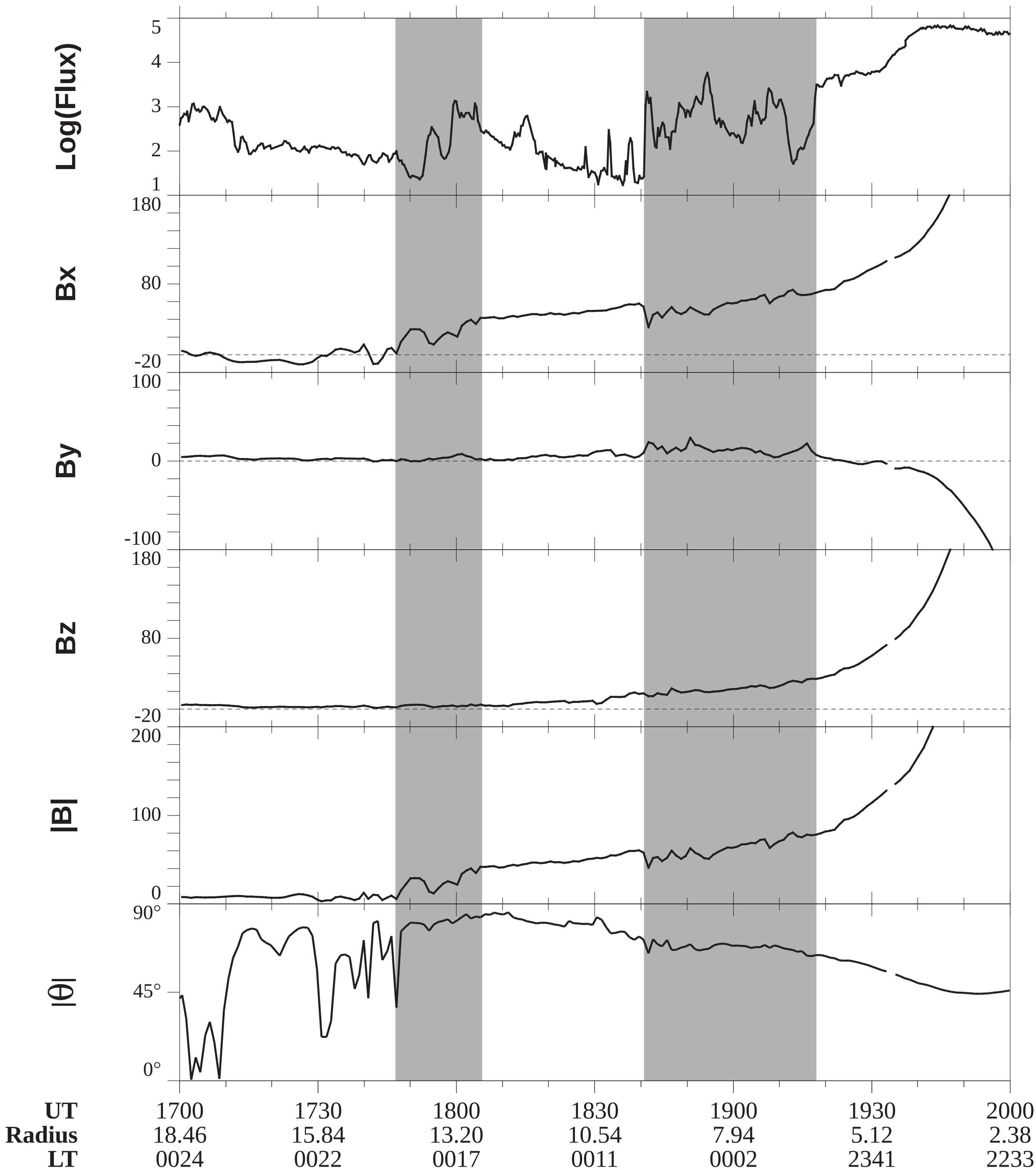

Log(Flux)
Bx
By
Bz
|B|
|θ|
5
4
3
2
1
180
80
-20
100
0
-100
180
80
-20
200
100
0
90°
45°
0°
UT
Radius
LT
1700
18.46
0024
1730
15.84
0022
1800
13.20
0017
1830
10.54
0011
1900
7.94
0002
1930
5.12
2341
2000
2.38
2233